Received: 3 August 2020 | Revised: 29 December 2020 | Accepted: 10 January 2021

DOI: 10.1111/jcpe.13424

Journal of Clinical Periodontology WILEY

CLINICAL INNOVATION REPORT

Ultrasonographic tissue perfusion analysis at implant and palatal donor sites following soft tissue augmentation: A clinical pilot study

Lorenzo Tavelli[1] | Shayan Barootchi[1] | Jad Majzoub[1] | Hsun-Liang Chan[1] | William V. Giannobile[1,2] | Hom-Lay Wang[1] | Oliver D. Kripfgans[2,3]

[1]Department of Periodontics & Oral Medicine, University of Michigan School of Dentistry, Ann Arbor, MI, USA

[2]Biointerfaces Institute and Department of Biomedical Engineering, College of Engineering, Ann Arbor, MI, USA

[3]Department of Radiology, University of Michigan Medical School, Ann Arbor, MI, USA

Correspondence
Hsun-Liang Chan, Department of Periodontics and Oral Medicine, University of Michigan School of Dentistry, 1011 North University Avenue, Ann Arbor, Michigan 48109-1078, USA.
Email: hlchan@umich.edu

Funding information
American Academy of Periodontology Sunstar Innovation Award, Grant/Award Number: AWD007224; Delta Dental Foundation, Grant/Award Number: AWD004687 and AWD010089; National Institute of Dental and Craniofacial Research, Grant/Award Number: 1R21DE027765–01A1 and 1R21DE029005-01A1; University of Michigan Department of Periodontics and Oral Medicine Clinical Research Grant, Grant/Award Number: N026036; National Center for Advancing Translational Sciences, Grant/Award Number: UL1TR000433

ABSTRACT

Aim: To describe the application of power Doppler Ultrasonography (US) for evaluating blood flow at implant and palatal donor sites following soft tissue augmentation with the connective tissue graft (CTG).

Materials and Methods: Five patients exhibiting a peri-implant soft tissue dehiscence received treatment with a coronally advanced flap and corresponding CTG. Power Doppler US was used for assessing blood volume at baseline, 1 week, 1 month, 6 months and 12 months post-surgery for assessing blood-flow dynamics at the implant and palatal donor sites. The speed-weighted and power-weighted colour pixel density (CPPD) were computed from colour velocity (CV) and colour power (CP), respectively.

Results: A mean increase in CV of 199.25% was observed at the midfacial region of the implant sites after 1 week compared to baseline. CV and CP were increased in all sites at 1 week and 1 month. At 6 and 12 months, the mean CV appeared lower than baseline at the implant sites. CCPD was increased at the palatal donor sites and at the great palatine foramen areas at the 1-week and 1-month post-operative evaluations.

Conclusions: Power Doppler US is a non-invasive and valuable tool for estimating tissue perfusion and CPPD variation during different phases of intra-oral soft tissue graft healing.

KEYWORDS
blood supply, blood-flow circulation, blood-flow velocity, connective tissue graft, dental implant, soft tissue augmentation, ultrasonography

1 | INTRODUCTION

Over the past decade, technological advancements have had major impact in dentistry by changing the way that oral health care is delivered. Non-ionizing, cross-sectional and real-time ultrasonography (US) is a promising imaging modality that serves as a valuable tool for evaluation of vital anatomical structures, and soft and hard tissue dimensions (Chan, Sinjab, et al., 2017; Bhaskar et al., 2018; Barootchi, Chan, et al., 2020; Chan & Kripfgans, 2020b). Recently, studies have validated the accuracy of US compared to histology or cone-beam computed tomography (Chan, Sinjab, et al., 2017; Chan et al., 2018; Tattan et al., 2019; Barootchi, Chan, et al., 2020). Another unique

advantage of US is the functional soft tissue evaluation, that is, blood flow and tissue perfusion. As different pathological states are characterized by altered vascularity in perfusion (Levy et al., 2008), perfusion estimation has been explored in medicine with numerous technologies. Among them, power Doppler US, a technique introduced to overcome the limitations of colour Doppler US (Rubin et al., 1994). This new scanning-angle independent approach integrates the colour flow power spectrum which extends the dynamic range and increases the machine's sensitivity to blood flow versus the traditional mean frequency estimator that is prone to noise for reduced flow (Rubin et al., 1994; Bude et al., 1994; Newman et al., 1994). In addition, power Doppler ultrasound has advantages for blood-flow (colour and power) quantification because of its ability to depict low-velocity signals and multidirectional flow and its lack of aliasing (Rubin et al., 1994; Welsh et al., 2019). To compensate for possible signal attenuation due to depth and tissue inhomogeneity, a method termed fractional moving blood volume (FMBV) has been established (Rubin et al., 1995; Welsh, 2004). This technique is based on the cumulative power distribution function to define a stable intra-vascular point, providing an absolute value for vascularity for inter- and intra-case comparisons (Rubin et al., 1997; Welsh et al., 2019). FMBV evaluation requires an offline image analysis technique applied to raw exported three-dimensional (3D) power Doppler US (Stevenson et al., 2015; Welsh et al., 2019). This method has been used to assess blood flow and perfusion of the kidney (Welsh et al., 2019), optic nerve (Vosborg et al., 2020), placenta (Lai et al., 2010) and foetal organs (Hernandez-Andrade, Thuring-Jonsson, et al., 2004; Hernandez-Andrade et al., 2007), among others.

It is possible that this non-invasive and real-time technology becomes an accurate and cost-effective tool for evaluating periodontal tissue perfusion. Detecting subclinical inflammation before the occurrence of periodontal or peri-implant bone loss could be one of the potential benefits of US (Chan & Kripfgans, 2020b). In addition, power Doppler US could also explore blood flow changes following soft tissue grafting, which might relate to the course of wound healing and the final clinical outcomes. In particular, blood volume analysis at grafted implant sites could provide further insight about the effect of phenotype modification on peri-implant health, as inflammation accompanies changes in tissue perfusion. The current clinical method of staging inflammation by "bleeding on probing" is subjective, and relative to implants still controversial (Hashim et al., 2018; Renvert et al., 2018; Barootchi, Ravida, et al., 2020). Another possible application of power Doppler US includes the evaluation of palatal donor site perfusion during different phases of wound healing. Having the advantages of being point-of-care, cost-efficient, and non-ionizing, US can become a convenient and an objective tool for research and for routine clinical practice for estimating tissue perfusion and possible would healing outcomes in research and clinical care arenas. Therefore, the aim of the present manuscript was to demonstrate the application of novel power Doppler US for assessing the alterations in blood flow and tissue perfusion at implant and palatal sites during the healing process after soft tissue augmentation with a connective tissue graft (CTG).

Clinical Relevance

Scientific rationale for the study: Non-ionizing, real-time ultrasonography (US) has shown to be a valuable tool for evaluating soft and hard tissues. Another advantage of US is the evaluation of blood flow and tissue perfusion with power Doppler ultrasonography. This technology is routinely used in medicine, however, its applicability in the oral cavity has not yet been explored to the best of our knowledge. This study describes a method for using US for assessing blood-flow variation in terms of colour and power pixel density (CPPD) at the implant and palatal donor sites following augmentation with connective tissue grafting procedures.

Principal findings: US power Doppler captured and estimate tissue perfusion at different time points at implant and palatal sites, with the 1-week and 1-month follow-up showing the greatest increase in CPPD. Blood volume at 6 and 12 months was reduced compared to baseline at the implant sites.

Practical implications: The use of US power Doppler is a non-invasive and suitable tool for estimating tissue perfusion and CPPD variation during different phases of wound healing. This method may become useful in the future in identifying conditions with abnormal blood flow or subclinical inflammation.

2 | CLINICAL INNOVATION REPORT

2.1 | Study registration, design and participants

Five periodontally and systemically healthy patients with aesthetic concerns regarding a dental implant diagnosed with peri-implant soft tissue dehiscence/deficiency (PSTD) (Zucchelli et al., 2019) requiring a treatment were selected from the Department of Periodontics and Oral Medicine, School of Dentistry, University of Michigan, Ann Arbor, USA. Further details of the inclusion and exclusion criteria are presented in the Appendix S1. The study was in accordance with the Institutional Review Board of the University of Michigan Medical School (HUM00140205) and was in accordance with the Declaration of Helsinki of 1975, revised in Tokyo in 2004.

2.2 | Surgical procedures

All surgical procedures were performed at the same clinic (Department of Periodontics and Oral Medicine, University of Michigan), by a single operator (L.T.). PSTDs were treated with an envelope split-full-split thickness coronally advanced flap (eCAF) + CTG as previously described by Zucchelli et al. (Zucchelli et al., 2013; Zucchelli et al., 2019). The CTGs were obtained as an epithelialized

gingival graft from the pre-molar areas on the palatal regions and were extraorally de-epithelialized. The palatal wounds were covered with a collagen dressing (Collatape, Zimmer Biomet) and secured with cross sutures (5/0 Vicryl, Ethicon, Johnson & Johnson). A few drops of cyanoacrylate tissue glue (PeriAcryl 90 HV, Glustitch) were applied over the palatal wounds on top of the collagen dressing (Tavelli et al., 2018; Tavelli, Ravida, et al., 2019). Pre-surgical procedures, surgical approaches and post-operative protocols are described in detail in the Appendix S1.

2.3 | Ultrasound images acquisition

The ultrasound equipment setup and the scanning procedures were performed by two experienced operators with expertise in the field of ultrasonography (H.C. and O.K.) (Chan, Sinjab, et al., 2017; Chan, Wang, et al., 2017; Tattan et al., 2019; Barootchi, Chan, et al., 2020; Chan & Kripfgans, 2020b). The scans were taken at baseline (prior to the initiation of the surgical procedure), and at 1-week, 1-month, 6-month and 12-month follow-up appointments at both the implant recipient and palatal donor sites. A commercially available ultrasound imaging device (ZS3, Mindray) as described in previous reports (Chan, Wang, et al., 2017; Barootchi, Chan, et al., 2020; Chan & Kripfgans, 2020b) coupled with a 24 MHz (64 μm axial image resolution) and miniature-sized (approximately 30 mm long, × 18 mm wide × 12 mm thick) probe prototype (L25–8) was used to generate ultrasound images (Figure 1).

As ultrasound is a real-time imaging modality, two types of images ("still" and "cine loops") were recorded and stored. A "still image" presents a single 2D image frame, while "cine loops" are videos that are generated as result of the collection of consecutive still images. Both image types were saved in the Digital Imaging and Communications in Medicine (DICOM) format. US "B-mode" generates 2D grey-scale images in which brightness is determined by the envelope of the returned echo signal. The strength of the echo signal depends on the mechanical properties of the involved soft and hard tissues (Figures 2 and 3).

US is either scattered or reflected. Structures much smaller than the acoustic wavelength (λ=64 μm) scatter the ultrasonic waves in all directions, whereas large structures reflect the ultrasonic wave obeying Snells' Law. (Chan & Kripfgans, 2020a).

"Colour flow" is an imaging mode in which the B-mode display is overlaid with additional colour pixels that represent detected blood flow. In this case B-mode provides an anatomical reference for the physical location of the detected blood flow (Chan & Kripfgans, 2020b). "Colour flow", also known as "colour Doppler", detects phase-changes in the received US signal. Red blood cells scatter US. Flowing red blood cells produce a scattered signal that changes in phase as long as the direction of the motion is non-perpendicular to the US beam. The largest phase-shift is seen when blood flows in the direction of the

FIGURE 1 FIGMiniature-sized probe prototype (L25–8). (a) Frontal view. (b) Lateral view. (c) Frontal view of the probe after its preparation for clinical use. (d) Ultrasound gel applied on the probe. (e) Clinical picture showing the application of the ultrasound probe at the midfacial aspect of an implant site (left central incisor) [Colour figure can be viewed at wileyonlinelibrary.com]

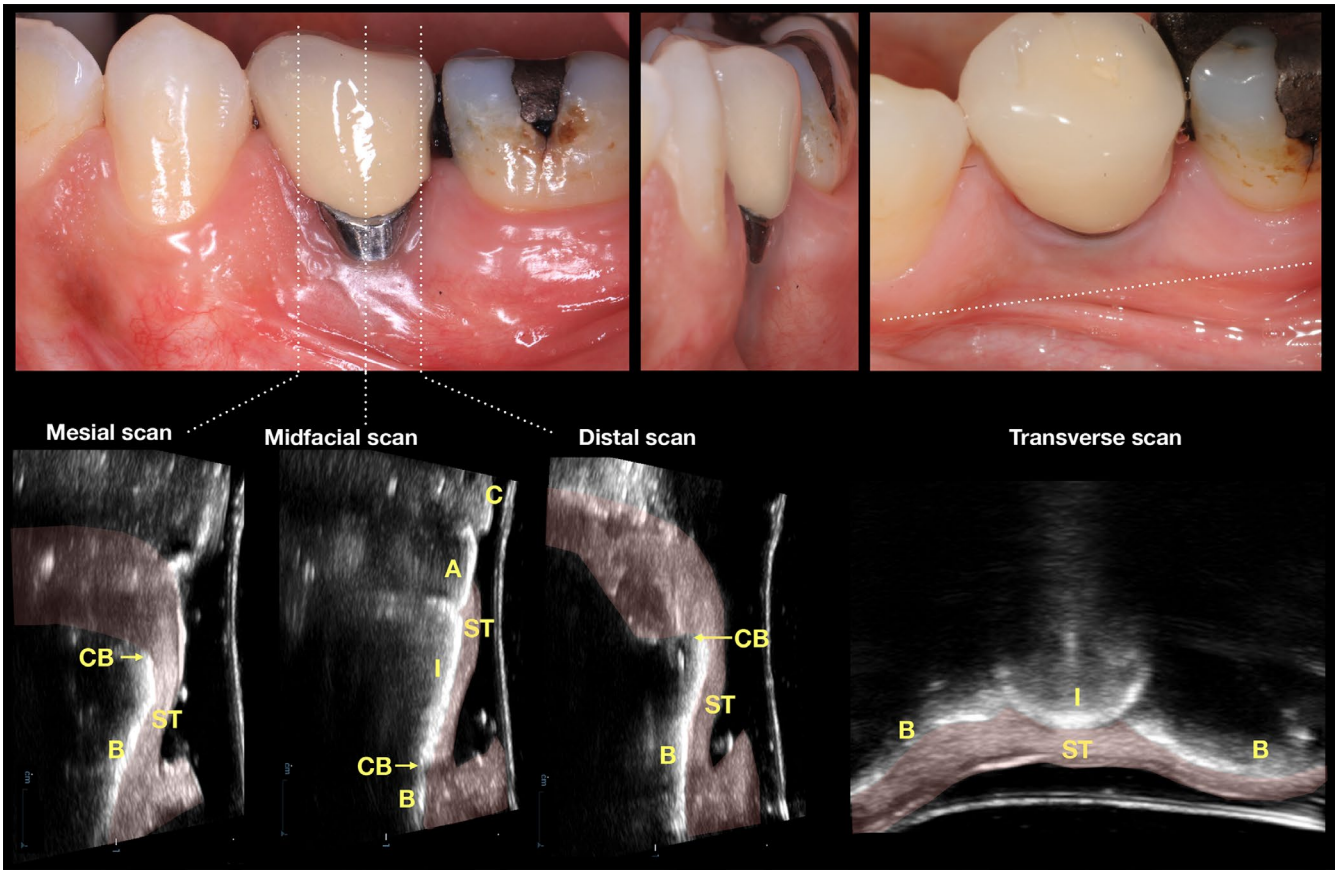

FIGURE 2 B-mode scan of the implant site showing the ultrasonographic imaging at the mesial-, midfacial-, distal- and transverse scan. Legend. A, abutment; B, bone plate; C, crown of the implant; CB, crestal bone; I, implant; ST, soft tissue [Colour figure can be viewed at wileyonlinelibrary.com]

FIGURE 3 B-mode scan of the palate showing the scan obtained 3-mm, 5-mm and 8-mm from the gingival margin of the second premolar prior to the harvesting. A scan in the region of the greater palatine foramen was also performed. Legend. GPF: greater palatine foramen; PB: palatal bone. ST: Soft tissue [Colour figure can be viewed at wileyonlinelibrary.com]

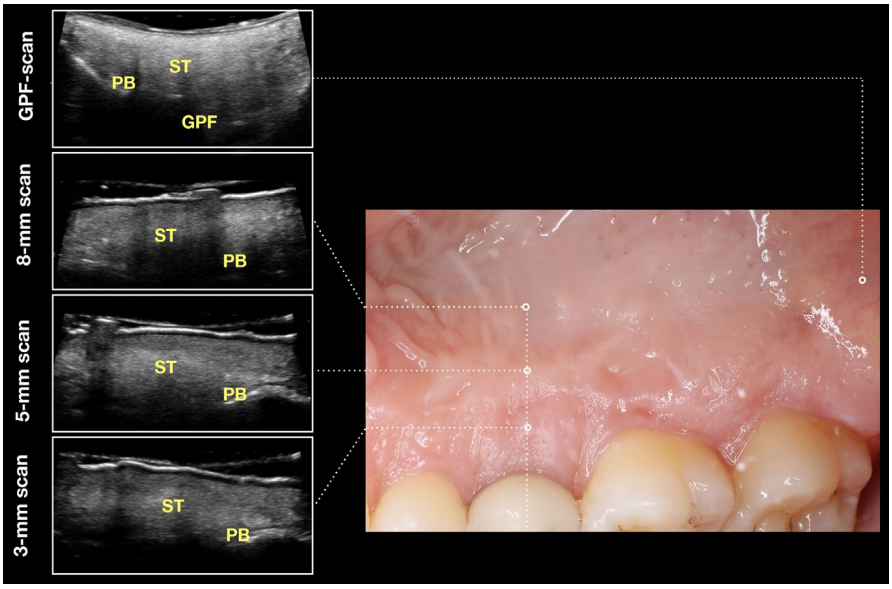

US beam and no phase-shift is observed when the flow is perpendicular to the beam. In particular, colour flow computes the mean phase change, that is, the mean velocity derived from the detected US signal. Therefore, colour flow mode utilizes colour Doppler signals, displaying blood-flow direction and relative velocity, with shades of red and blue colours assigned to image pixels based on the flow direction and velocity. In particular, the colour red indicates blood flow towards the transducer, while blue colour denotes blood flow in the opposite direction (Figure 4). Lack of colour pixels can be interpreted as either no blood flow or blood flow perpendicular to the US beam. Live scanning allows the operator to position the US probe in a way that is most representative of the given vascular anatomy.

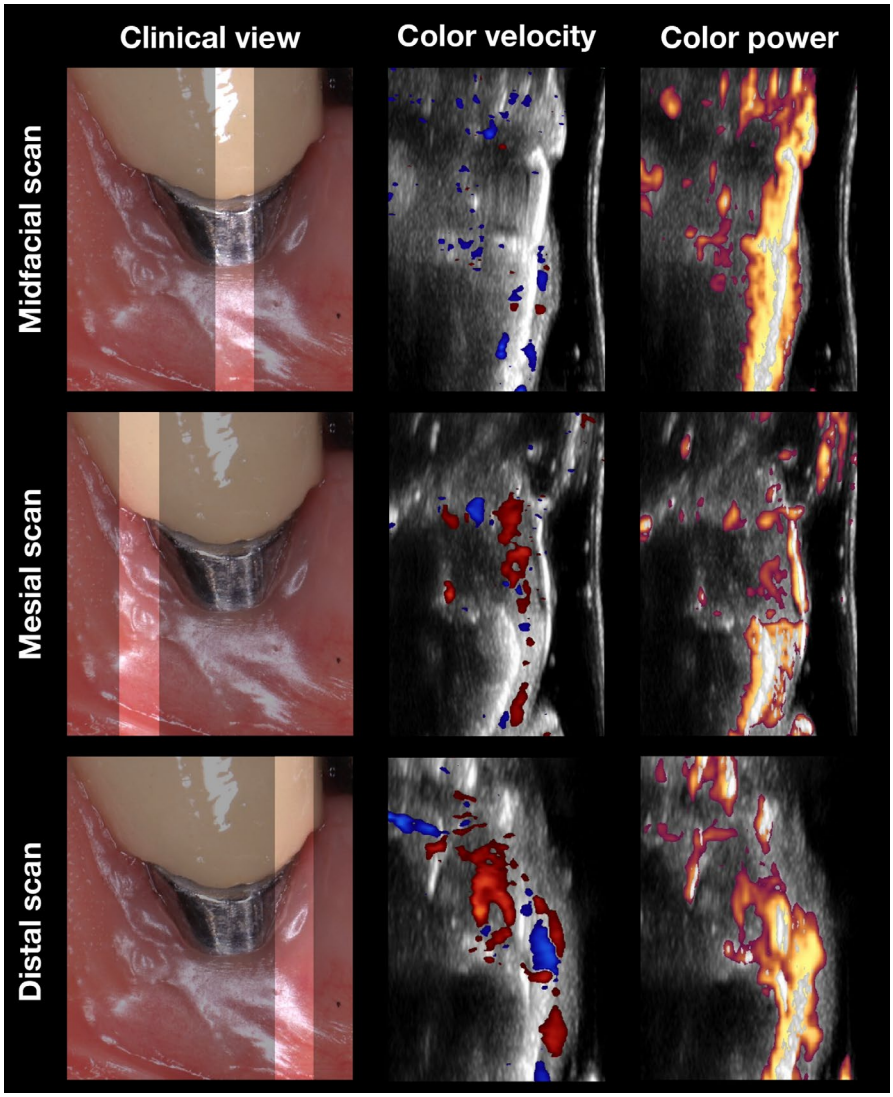

FIGURE 4 Colour velocity and colour power at the midfacial, mesial and distal scans. The displayed colour velocity visualizes the speed at which blood flows, while colour power shows the amount of blood flowing within the lumens in the field of view. Colour velocity imaging was performed using a constant velocity scale (±2.3 cm/s), with the colour red indicating blood flow towards the transducer, and the blue colour denotes blood flow in the opposite direction. Colour power is displayed in a single-hue red colour [Colour figure can be viewed at wileyonlinelibrary.com]

The displayed colour velocity (CV) is the projection of the actual velocity onto the US beam, which mathematically equals the multiplication of the true velocity by the cosine of the angle to the US beam. CV data are filtered using a "wall filter" to eliminate tissue motion of the adjacent vascular walls (Chan & Kripfgans, 2020b). CV visualizes the speed at which blood flows within the lumens in the field of view. For higher tissue perfusion higher velocities might be observed. "Colour power" (CP) is an imaging mode that is also based on detecting phase-change of the received US signal. However, instead of displaying the mean velocity, it displays the integrated power of the received US signal after the wall filter has been applied. This power is displayed in a single-hue red colour (Figure 4). Since the power is derived after the wall filter has been applied, CP visualizes the *amount* of blood flowing within the lumens in the field of view and it is particularly useful for small vessels and those with low-velocity flow. For higher tissue perfusion, more blood vessels might be active, and the vasculature might also show vasodilation, thus more blood might be flowing.

2.4 | Areas of interest

The areas of interest at the implant site were: (a) midfacial, (b) mesial (at the line angle between the crown and the mesial papilla), (c) distal (at the line angle between the crown and the distal papilla) and (d) transverse scan at 3 mm from the mucosal margin level (Chan & Kripfgans, 2020b). For the midfacial, mesial and distal scans, the US probe was oriented parallel to the long axis of the implant and perpendicular to the occlusal plane, while for the transverse scan the probe was oriented parallel to the occlusal plane. The areas of interest at the palatal donor site were: 3-, 5-, and 8-mm reference points apical to the gingival margin of the first and second pre-molars, and the greater palatine foramen (GPF) area, which was identified by palpation at the junction between the horizontal plate of the maxilla and alveolar ridge at the 3rd molar location (Fu et al., 2011; Tavelli, Barootchi, et al., 2019). For each area of interest at the implant and palatal site, B-mode, CV and CP scans were performed and saved as still images (for the B-mode) and cine loop videos (for CV and CP modes) at the baseline, 1 week, 1 month, 6-months and 12-months.

2.5 | Ultrasound image analysis and blood volume calculation

As a preliminary analysis, ultrasonography measurements were taken of the mucosal recession depth (MRec), mucosal thickness (MT) and palatal thickness (PT) on the B-mode images using a commercially available software package (Horos™, version 3.3.6, Horos Project), as previously described (Chan & Kripfgans, 2020b). All the measurements were carried out by a single calibrated and experienced examiner (J.M.) who is an active member of the dental ultrasonography laboratory and has been conducting extensive US periodontal/peri-implant measurements for the past 2 years. Additional details are also listed in the Appendix S1.

The speed-weighted colour pixel density and power-weighted colour pixel density (CPPD) was computed from CV and CP, respectively. For such, a ROI on the soft tissue of interested was identified. For the implant site, the ROI was defined as the area between the soft tissue margin and extending 7 mm apically, while for the palatal scans, the entire the soft tissue above the palatal bone was used as ROI (Figure 5). The colour pixel information from within the ROI were extracted using the displayed colour- and power-bar to decode the underlying velocities and power (Chan & Kripfgans, 2020b).

It should be noted that colour velocity imaging was performed using a constant velocity scale (±2.3 cm/s) to maintain the same wall filter for all cases. This opens the possibility for aliasing in the colour velocity image, that is, velocities larger than +2.3 cm/s or smaller than −2.3 cm/s, will lead to the positive/negative velocity scale, respectively. Affects to the speed-weighted colour pixel density is, however, minimized by using the absolute measured velocities, that is, negative velocities are negated to obtain positive velocities. The CV and CP gain was also kept the constant throughout the study in order to warrant sensitivity (velocity and power) and to ease the comparison of velocity power values from individual scans and patients.

Speed-weighted (CV_w) and power-weighted (CP_w) colour pixel densities were computed by a calibrated examiner with expertise in ultrasound imaging and image/signal processing (O.K.) using custom scripts for Matlab (The Mathworks, Natick, MA) (Video S1). All data were processed using the same scripts to improve scientific rigor and eliminate bias.

CV_m and CP_m were obtained as an average of CV/CP_w across at least 5 the cardiac cycles (6 second cine clips at minimum 20 Hz frame rate for cardiac averaging). The variation in percentages compared to baseline was computed and descriptive statistics were used to present the gathered data as means ± standard deviations (SD).

3 | RESULTS

3.1 | Experimental population and baseline characteristics

Five female patients (mean age 52.2 ± 11.1 years), each with a single PSTD were consecutively treated with an eCAF +CTG. All PSTDs extended until the abutment component alone, without exposure of the implant fixtures to the oral cavity. Baseline characteristics and blood volume before the surgery (baseline) are depicted in Tables 1 and 2 and in the Appendix S1.

3.2 | Imaging interpretation

Figure 2 showed representative US images taken in the abovementioned 4 locations. In the midfacial slice, the implant-supported crown surface appeared as a hyperechoic (bright) band with relatively uniform (apparent) thickness along its length. The abutment surface, also a hyperechoic structure, followed the crown in an apical position. The implant fixture surface was also visible as a

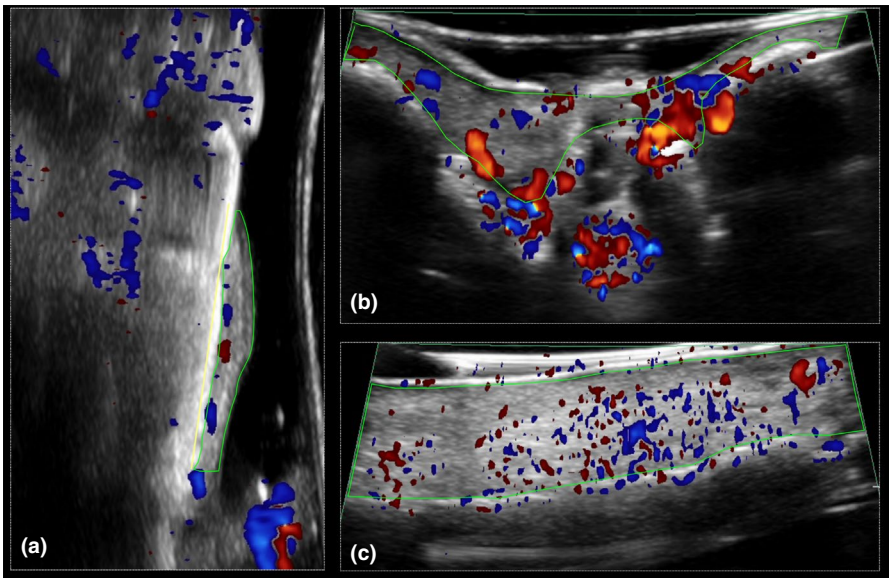

FIGURE 5 Definition of the region of interest (ROI) at the midfacial (a) and transverse (b) scans of the implant site and at the 5-mm palatal scan (c). The ROI includes the soft tissue component only, with the same anatomical references that are using to define the ROI at different time points [Colour figure can be viewed at wileyonlinelibrary.com]

TABLE 1 Characteristics of patients at baseline and ultrasonographic analysis at the implant sites

Variable	Baseline characteristics
Age (mean ± SD) (years)	52.2 ± 11.1
Sex (M/F)	0/5
Smokers (*n*)	1 (4 cigarettes/day)
Sites	1 maxillary central incisor, 1 maxillary lateral incisor and 3 mandibular premolars
PSTD class IIa	1
PSTD class IIb	4
PD (mean ± SD) (mm)[b]	2.7 ± 0.6
MRec (mean ± SD) (mm)[a]	1.97 ± 0.39
MT at 1 mm (mean ± SD) (mm) [a]	0.69 ± 0.26
MT at 3 mm (mean ± SD) (mm)[a]	1.2 ± 0.2
MT at 5 mm (mean ± SD) (mm)[a]	1.39 ± 0.76
CPPD Midfacial (mean ± SD) (cm/s and fractional-pixel)[a]	0.12 ± 0.04 (CV)/0.54 ± 0.08 (CP)
CPPD Mesial (mean ± SD) (cm/s and fractional-pixel)[a]	0.15 ± 0.06 (CV) / 0.59 ± 0.09 (CP)
CPPD Distal (mean ± SD) (cm/s and fractional-pixel)[a]	0.16 ± 0.05 (CV) / 0.61 ± 0.09 (CP)
CPPD Transverse (mean ± SD) (cm/s and fractional-pixel)[a]	0.13 ± 0.04 (CV) / 0.58 ± 0.08 (CP)

Abbreviations: cm, centimetre; CP, colour power; CPPD, colour and power pixel density; CV, colour velocity; F, Female; M, male; mm, millimetre; MRec, Mucosal recession depth; MT, mucosal thickness; n, number; PD, probing depth; PSTD, peri-implant soft tissue dehiscence/deficiency; SD, standard deviation.

[a]measured with ultrasound.

[b]measured using a periodontal probe (PCP UNC 15, Hu-Friedy, Chicago, USA).

TABLE 2 Baseline characteristics and blood volume at the palatal donor site

Variable	3-mm scan	5-mm scan	8-mm scan	GPF scan
Palatal thickness (mean ± SD) (mm)	3.49 ± 0.36	4.13 ± 0.67	4.48 ± 0.67	5.98 ± 0.84
CV (mean ± SD) (cm/s)	0.14 ± 0.05	0.17 ± 0.07	0.18 ± 0.1	0.18 ± 0.09
CP (mean ± SD) (fractional-pixel)	0.62 ± 0.08	0.62 ± 0.11	0.61 ± 0.08	0.64 ± 0.11

Abbreviations: cm, centimetre; CP, colour power; CV, colour velocity; GPF, greater palatine foramen; mm, millimetre; s, second; SD, standard deviation.

uniform hyperechoic band, with possible thread appearance if exposed. The bone surface was identifiable as a bright curved line. The peri-implant mucosa appeared as a hypoechoic (dark) band surrounding the abutment, implant fixture and bone. The mesial and distal scans showed the interproximal soft tissue between the bone crest and the papilla tip. The transverse scan showed the implant abutment in the middle of the image as a hyperechoic semi-circular structure, the facial alveolar bone surface in front of the two adjacent teeth, and the investing hypoechoic overlying soft tissues. The palatal scans showed hypoechoic palatal mucosa between the two hyperechoic lines running relatively parallel between them. The superior hyperechoic line is the soft tissue surface, while the inferior represents is the palatal bone. A similar imaging was observed at the GPF area, except for the soft tissue shaping as a funnel at the foramen site through which the neurovascular bundles leave the oral cavity for the pterygopalatine fossa. The palatal bone showed as a discontinued bright line at the foramen location.

Blood flow was seen as "cine loop" videos generated by the collection of consecutive image frames where the B-mode display is overlaid with colour pixels (Video S2). Colour Doppler cine loops display blood velocity, with shades of red and blue colours, while the colour power cine loops show the blood volume in the area of interest as a single-hue red colour. The overlaid implant or palatal structures observed in the B-mode provide anatomical references for the blood velocity and volume image interpretation.

3.3 | Blood volume changes at the implant site

In the midfacial scan, an increase in CV_m of 199% was observed compared to baseline at the 1-week follow-up. The CV_m increase in the mesial, distal and transverse scans were 102%, 95.6% and 163%, respectively, compared to baseline. The CV_m increase at 1 month was similar to the one observed at 1 week in all the scans. At the 6- and 12-month follow-up, CV_m was found to be lower than baseline (Figure 6). A similar trend was observed for CP_m change over time (Table 3 and Appendix S1).

3.4 | Blood volume change at the palatal donor site

At the 1-week follow-up, the CV_m change was 146% at the 3-mm scan, while the 5-mm and 8-mm scan showed a CV_m increase of

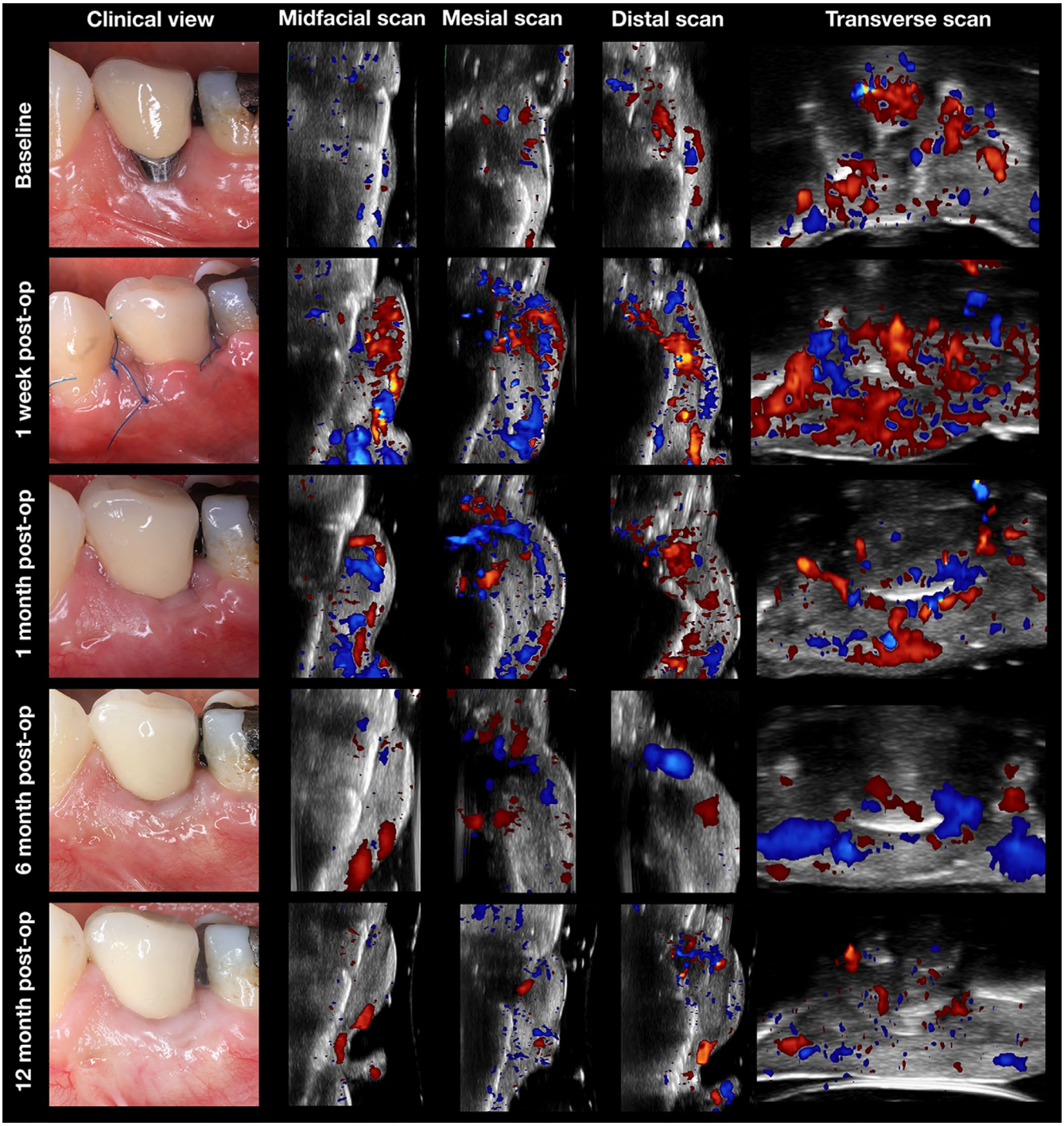

FIGURE 6 Ultrasound colour mode at the implant site at the midfacial, transverse, mesial and distal scan, showing the variation in colour velocity at baseline, 1-week, 1-month, 6-month and 12-month post-op [Colour figure can be viewed at wileyonlinelibrary.com]

179% and 222%, respectively, compared to baseline. The CV_m increase at 1-month was found to be still higher than baseline values in all the scans. At the 6- and 12-month recalls, similar CV_m change were found in the 3-, 5- and 8-mm scans, with minimal differences compared to baseline CV_m. The CV_m at the GPF area showed an increase of 50.1% after 1 week, 40.8% after 1 month, 11.8% after 6 months and 4.81% after 12 months (Figure 7). Table 4 and Appendix S1 depict CV_m and CP_m over the 12-month observation period at the palatal site.

4 | DISCUSSION

Power Doppler US has grown to be a full portion of diagnostics across a diversity of medical specialties, in particular for distinguishing normal from abnormal blood flow (Hansen et al., 2017; Goddi et al., 2017; Oglat et al., 2018; Pinter et al., 2018; Welsh et al., 2019). Its application in dentistry and in particular in periodontics can also prove beneficial with exploring blood flow alterations around natural teeth and dental implant in a non-ionizing, chair-side and cost-efficient manner with potential implications such as detecting pathological conditions, or identifying an undetectable subclinical inflammation prior to the detection of bone loss (Chan & Kripfgans, 2020b).

Earlier studies examined the vascular morphology and blood flow in healthy, or inflamed or diseased periodontia (Kennedy, 1974; Hock, 1979; Kaplan et al., 1982; Hock & Kim, 1987). They showed that induction of inflammation resulted in the development of collateral circulation from the periodontal ligament to the gingiva (Kennedy, 1974), that could explain the increased blood flow in the presence of gingivitis (Hock & Kim, 1987) or periodontal disease (Kaplan et al., 1982). In particular, sites with moderate to severe periodontitis demonstrated a much greater blood flow (250–400%) than sites with minimal periodontal destruction (Kaplan et al., 1982). Nevertheless, their method of using radiolabeled carbonized microspheres infused into the left cardiac ventricle (Kaplan et al., 1982; Hock & Kim, 1987) is not reproducible in human clinical studies, nor possible during standard clinical patient-care procedures. Some authors have evaluated gingival perfusion using laser-Doppler flowmetry (Mavropoulos et al., 2001; Ambrosini et al., 2002; Patino-Marin et al., 2005; Retzepi et al., 2007; Kuraji et al., 2020). However, some limitations of this technology may include the presence of motion artifact noise, lack of quantitative units for perfusion, limited diagnostic values in smokers, and lack of studies validating this tool in periodontics (Firkova & Bouka, 2019). Fluorescein angiography has also been utilized for assessing capillary blood microcirculation after mucogingival and soft tissue grafting procedures (Mormann et al., 1975; Mormann & Ciancio, 1977; Burkhardt & Lang, 2005). Nevertheless, some of the drawback can be the prerequisite of intravenous injection of a contrast medium, progressive dye leakage that may lead to loss of vascular details, and possible side effects such as vertigo, nausea, vomiting or anaphylaxis (Burkhardt & Lang, 2005; Keane & Sadda, 2010).

The present study aimed at describing an US-based colour and power pixel density (CPPD) technique for assessing blood flow and tissue perfusion changes at implant and palatal sites following connective tissue grafting procedures. While this method is well-validated in the medical field (Hernandez-Andrade, Jansson, et al., 2004; Gao et al., 2013; Welsh et al., 2019), to the best of our knowledge, this is the first report of its application in Periodontics. Among the advantages of ultrasonography compared to other technologies previously utilized for assessing tissue perfusion in natural dentition, it has to be mentioned that power Doppler US allows for a non-ionizing, chair-side and real-time evaluation of blood flow and its variation over time. Despite the pilot nature of the current article and the limited sample size we observed a mean increase in blood volume at 1 week and 1 month compared to baseline values. Interestingly, at the 6- and 12-month follow-up we noticed a reduction in the mean blood flow. If these findings are confirmed in future studies, it will be possible to speculate that the decrease of subclinical inflammation compared to baseline could have been related to surgical interventions that modify the soft tissue peri-implant phenotype (Roccuzzo et al., 2016; Perussolo et al., 2018; Tavelli, Barootchi, Avila-Ortiz, et al., 2020) or that participating in this study with frequent follow-up visits may have had a positive impact on patients' motivation and oral hygiene levels resulting in a significantly decreased mucosal inflammation.

Two previous studies evaluated blood flow following soft tissue grafting (Demirkol et al., 2001; Tatarakis et al., 2018). Demirkol et al.

TABLE 3 Changes in colour velocity and colour power over the 12-month observation period at implant sites

	Colour velocity change (mean ± SD) (%)				Colour power change (mean ± SD) (%)			
Time intervals	Midfacial scan	Mesial scan	Distal scan	Transverse scan	Midfacial scan	Mesial scan	Distal scan	Transverse scan
T_1–T_0	199 ± 45.6	102 ± 49.8	95.6 ± 40.9	163 ± 75.8	48.6 ± 27.1	21.8 ± 2.8	17.4 ± 7.13	32.2 ± 5.55
T_2–T_0	153 ± 44.3	97.9 ± 57.4	95.8 ± 54.3	146.9 ± 76.8	58.89 ± 38.6	33.5 ± 14.9	20.4 ± 5.14	56.1 ± 8.14
T_3–T_0	−31.5 ± 13.5	−11.8 ± 5.34	−23.6 ± 6.63	−17.5 ± 9.23	−9.27 ± 11.2	−8.54 ± 5.29	−14.2 ± 8.49	−4.48 ± 11.5
T_4–T_0	−34.2 ± 29.7	−8.93 ± 23.1	−5.48 ± 8.87	−2.47 ± 28.9	−12.5 ± 6.25	−10.9 ± 10.4	−12.1 ± 10.6	−6.80 ± 7.31

The changes were computed by subtracting the colour velocity or colour power at a follow-up time point to the respective value at baseline. Negative colour velocity or colour power changes indicate a reduction in the blood volume at the follow-up compared to baseline.

Abbreviations: CP, colour power; CV, colour velocity; SD, standard deviation; T_0, baseline; T_1, 1-week post-op; T_2, 1-month post-op; T_3:6-month post-op; T_4, 12-month post-op.

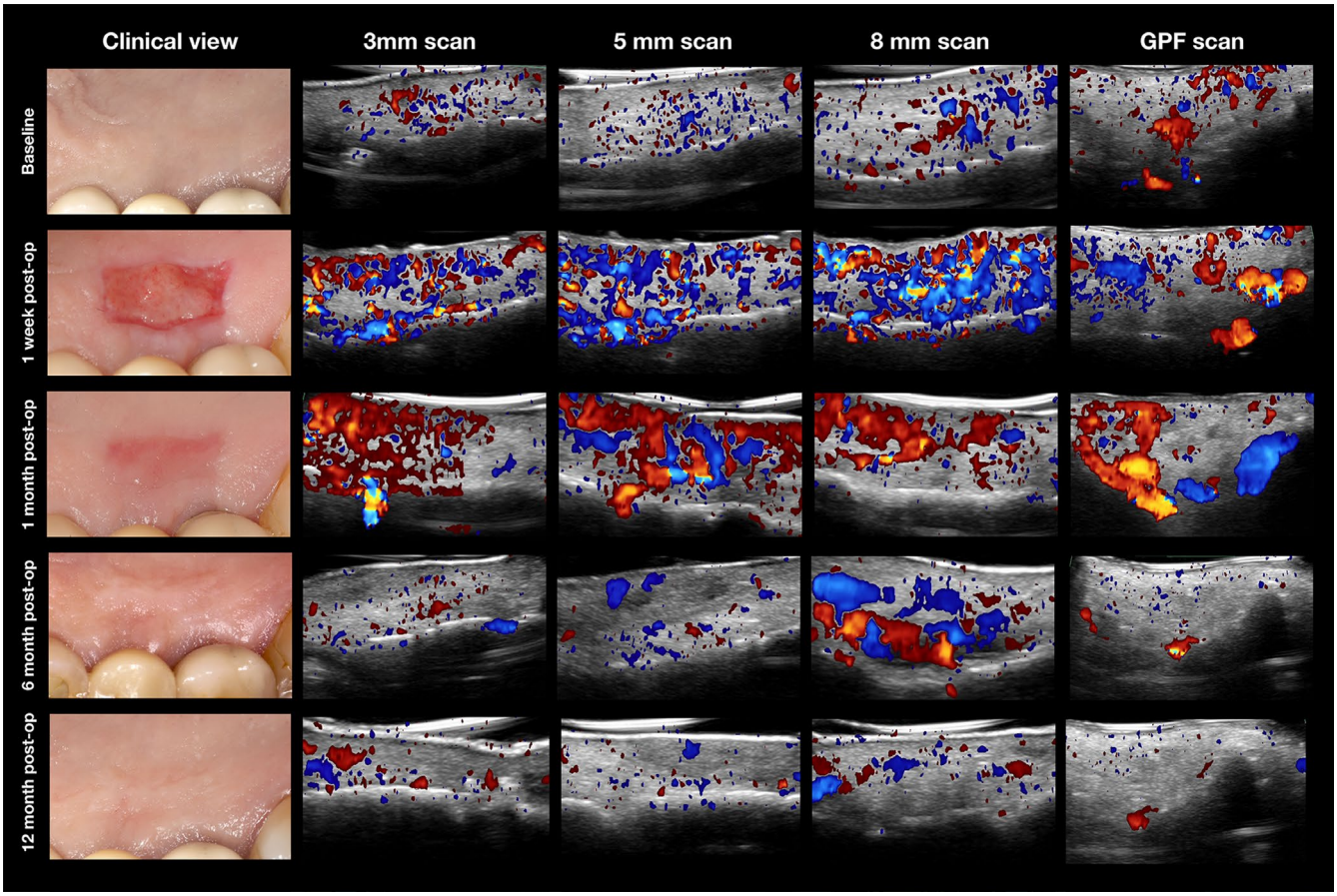

FIGURE 7 Ultrasound colour mode at the palatal sites at different time points. An increase in blood volume was observed in all the scans (3 mm, 5 mm, 8 mm and greater palatal foramen [GPF]) at the 1-week and 1-month follow-up, compared to baseline [Colour figure can be viewed at wileyonlinelibrary.com]

TABLE 4 Colour velocity and colour power variation over the 12-month observation period at the palatal site

	Colour velocity change (mean ± SD) (%)				Colour power change (mean ± SD) (%)			
Time intervals	3 mm scan	5 mm scan	8 mm scan	GPF scan	3 mm scan	5 mm scan	8 mm scan	GPF scan
T_1–T_0	146 ± 62.7	179 ± 84.7	222 ± 40.9	50.1 ± 22.4	39.9 ± 10.6	39.3 ± 19.7	44.5 ± 15.7	19.8 ± 3.50
T_2–T_0	185 ± 68.7	127 ± 59.6	178 ± 83.1	40.8 ± 22.5	37.2 ± 24.2	39.4 ± 26.8	28.8 ± 14.4	20.9 ± 10.7
T_3–T_0	5.84 ± 6.19	9.11 ± 7.29	7.84 ± 7.18	11.8 ± 9.36	3.91 ± 5.84	1.78 ± 6.75	4.92 ± 1.79	4.16 ± 6.43
T_4–T_0	4.58 ± 14.7	4.64 ± 15.9	2.53 ± 9.05	4.81 ± 9.98	0.790 ± 5.16	−1.69 ± 4.34	7.51 ± 6.95	1.31 ± 9.83

The changes were computed by subtracting the colour velocity or colour power at follow-up to the respective value at baseline and calculating the percentage of this difference compared to the baseline value. Negative colour velocity or colour power changes indicate a reduction in the blood volume at the follow-up compared to baseline.

Abbreviations: CP, colour power; CV, colour velocity; SD, standard deviation; T_0, baseline; T_1, 1-week post-op; T_2, 1-month post-op; T_3:6-month post-op; T_4, 12-month post-op.

used a xenon-133 clearance method for assessing blood circulation of free gingival grafts during the initial healing phase, showing that mean blood flow gradually increased at 10 and 20 days before reaching the initial value of the recipient area on the day 40 (Demirkol et al., 2001). Using laser-Doppler flowmetry, Tatarakis et al. found that collagen matrix and CTG displayed a differing pattern of blood-flow changes over time (Tatarakis et al., 2018). Due to the preliminary nature of this study, no efforts were made for performing direct or indirect comparisons between our findings and blood volume variation obtained with different technologies.

In addition, soft tissue wound healing around dental implants differs from the healing process observed in the natural dentition, with the peri-implant soft connective tissue that resembles a scar in composition, fibre orientation and vasculature (Sculean et al., 2014). Most of the blood supply of the peri-implant mucosae are provided by supraperiosteal plexuses that divides into several branches running towards the abutment surface, with the least number of vessels found close to the implant surface (Buser et al., 1992; Berglundh et al., 1994; Sculean et al., 2014). This difference in the vasculature may affect the pattern of blood volume changes during the healing compared to natural dentition.

A previous study by Molnar and co-workers evaluated blood-flow changes following the single-incision palatal harvesting technique with Laser Speckle Contrast Imaging showing a strong correlation between reperfusion time and healing score (Molnar et al., 2019). Our study evaluated the CPPD of the palatal donor site following free gingival graft harvesting, which has slowly become a popular technique among clinicians (Tavelli, Ravida, et al., 2019; Tavelli, Barootchi, Avila-Ortiz, et al., 2020; Barootchi, Tavelli, et al., 2020). The peak of CV_m was observed at 1 week for all the examined scans, with the 8-mm area displaying higher values of blood volume compared to the other palatal sites. This is in line with a cadaver study showing that a higher mean number of medium and large vessels are found in the deep palate (Tavelli, Barootchi, Namazi, et al., 2020). It is important to highlight that even though the harvesting was performed in the pre-molar regions, the greater palatine artery at the area of the GPF showed an increase in blood volume at both 1-week and 1-month. This finding is in agreement with the observations from a recent wound healing model, showing major changes in the vascular network in the whole region following an injury, with the blood supply redirected to the wounded area (Yousefi et al., 2014). The increase in vessel diameters and the enlargement of the recruited collateral bridges mediate the enhancement of the blood flow, which is vital for the healing and surviving of the injured tissue (Yousefi et al., 2014).

Among the limitations of the present pilot study, the inclusion of a single light smoker (even though CPPD variations at the implant- and palatal donor site did not show a substantial difference compared to the other subjects) have to be noted. In addition, although the presented method has already been shown to be reliable and it has been validated in the medical field (Carson et al., 1998; Fleischer et al., 1999; Hernandez-Andrade, Jansson, et al., 2004; Gao et al., 2013; Welsh et al., 2019), future studies comparing power Doppler US and other techniques, such as fluorescein angiography or laser-Doppler flowmetry, for tissue perfusion evaluation at implant and palatal sites are needed. Future studies may benefit from power Doppler US for evaluating tissue perfusion during different phases of periodontal/peri-implant healing, diagnosis of pathological conditions or subclinical inflammation. Definition of blood-flow thresholds for health vs inflammatory or infective processes, based also on patient's characteristics and anatomical location, are therefore encouraged.

5 | CONCLUSIONS

A novel ultrasound power Doppler method was developed to estimate tissue perfusion and CPPD variation, which correlates well with the course of normal oral wound healing events. Once validated, this technology can become an objective, non-ionizing and chair-side method to study wound repair dynamics and tissue perfusion.

ACKNOWLEDGEMENTS

The study was supported by grants from the National Institute of Dental and Craniofacial Research (NIDCR) R21 grant (1R21DE027765 – 01A1 and 1R21DE029005-01A1), National Center for Advancing Translational Sciences of the National Institutes of Health Award (UL1TR000433), Delta Dental Foundation (AWD010089 and AWD004687), American Academy of Periodontology Sunstar Innovation Award (AWD007224), and University of Michigan Department of Periodontics and Oral Medicine Clinical Research Grant (N026036).

CONFLICT OF INTEREST

The authors do not have any financial interests, either directly or indirectly, in the products or information enclosed in the paper.

AUTHOR CONTRIBUTIONS

L.T., S.B., H.L.C., W.V.G, H.L.W. and O.D.K. contributed to the conception and design of the work. L.T., H.L.C. and J.M. contributed to the collection of the data, O.D.K. computed the data and S.B. analysed the data. L.T., S.B., H.L.C and O.D.K. designed the schematic illustrations. L.T., S.B., and O.D.K led the writing; H.L.C., W.V.G, J.M. and H.L.W. critically reviewed and contributed to the writing of the manuscript.

DATA AVAILABILITY STATEMENT

The data that supports the finding of this study are available in the supplementary material of this article.

ORCID

Lorenzo Tavelli https://orcid.org/0000-0003-4864-3964
Shayan Barootchi https://orcid.org/0000-0002-5347-6577
Hsun-Liang Chan https://orcid.org/0000-0001-5952-0447
William V. Giannobile https://orcid.org/0000-0002-7102-9746
Hom-Lay Wang https://orcid.org/0000-0003-4238-1799

REFERENCES

Ambrosini, P., Cherene, S., Miller, N., Weissenbach, M., & Penaud, J. (2002). A laser Doppler study of gingival blood flow variations following periosteal stimulation. *Journal of Clinical Periodontology*, *29*, 103–107. https://doi.org/10.1034/j.1600-051x.2002.290203.x

Barootchi, S., Chan, H. L., Namazi, S. S., Wang, H. L., & Kripfgans, O. D. (2020). Ultrasonographic characterization of lingual structures pertinent to oral, periodontal, and implant surgery. *Clin Oral Implants Res*, *31*(4), 352–359. https://doi.org/10.1111/clr.13573

Barootchi, S., Ravida, A., Tavelli, L., & Wang, H. L. (2020). Nonsurgical treatment for peri-implant mucositis: A systematic review and meta-analysis. *Int J Oral Implantol (Berl)*, *13*, 123–139.

Barootchi, S., Tavelli, L., Zucchelli, G., Giannobile, W. V., & Wang, H. L. (2020). Gingival phenotype modification therapies on natural teeth: A network meta-analysis. *Journal of Periodontology*, *91*(11), 1386–1399. https://doi.org/10.1002/JPER.19-0715

Berglundh, T., Lindhe, J., Jonsson, K., & Ericsson, I. (1994). The topography of the vascular systems in the periodontal and peri-implant tissues in the dog. *Journal of Clinical Periodontology*, *21*, 189–193. https://doi.org/10.1111/j.1600-051x.1994.tb00302.x

Bhaskar, V., Chan, H. L., MacEachern, M., & Kripfgans, O. D. (2018). Updates on ultrasound research in implant dentistry: A systematic review of potential clinical indications. *Dentomaxillofac Radiol*, *47*, 20180076. https://doi.org/10.1259/dmfr.20180076

Bude, R. O., Rubin, J. M., & Adler, R. S. (1994). Power versus conventional color Doppler sonography: Comparison in the depiction of

normal intrarenal vasculature. *Radiology*, *192*, 777–780. https://doi.org/10.1148/radiology.192.3.8058946

Burkhardt, R., & Lang, N. P. (2005). Coverage of localized gingival recessions: Comparison of micro- and macrosurgical techniques. *Journal of Clinical Periodontology*, *32*, 287–293. https://doi.org/10.1111/j.1600-051X.2005.00660.x

Buser, D., Weber, H. P., Donath, K., Fiorellini, J. P., Paquette, D. W., & Williams, R. C. (1992). Soft tissue reactions to non-submerged unloaded titanium implants in beagle dogs. *Journal of Periodontology*, *63*, 225–235. https://doi.org/10.1902/jop.1992.63.3.225

Carson, P. L., Fowlkes, J. B., Roubidoux, M. A., Moskalik, A. P., Govil, A., Normolle, D., LeCarpentier, G., Nattakom, S., Helvie, M., & Rubin, J. M. (1998). 3-D color Doppler image quantification of breast masses. *Ultrasound in Medicine and Biology*, *24*, 945–952. https://doi.org/10.1016/s0301-5629(98)00055-6

Chan, H. L., & Kripfgans, O. D. (2020a). Examination, diagnosis and treatment outcome evaluation. (Albert) Chan Hsun-Liang & D. Kripfgans Oliver In: *Dental Ultrasound in Periodontology and Implantology*. Springer International Publishing.

Chan, H. L., & Kripfgans, O. D. (2020b). Ultrasonography for diagnosis of peri-implant diseases and conditions: A detailed scanning protocol and case demonstration. *Dentomaxillofac Radiol*, *49*(7), 20190445. https://doi.org/10.1259/dmfr.20190445

Chan, H. L., Sinjab, K., Chung, M. P., Chiang, Y. C., Wang, H. L., Giannobile, W. V., & Kripfgans, O. D. (2017). Non-invasive evaluation of facial crestal bone with ultrasonography. *PLoS One*, *12*, e0171237. https://doi.org/10.1371/journal.pone.0171237

Chan, H. L., Sinjab, K., Li, J., Chen, Z., Wang, H. L., & Kripfgans, O. D. (2018). Ultrasonography for noninvasive and real-time evaluation of peri-implant tissue dimensions. *Journal of Clinical Periodontology*, https://doi.org/10.1111/jcpe.12918

Chan, H. L., Wang, H. L., Fowlkes, J. B., Giannobile, W. V., & Kripfgans, O. D. (2017). Non-ionizing real-time ultrasonography in implant and oral surgery: A feasibility study. *Clin Oral Implants Res*, *28*, 341–347. https://doi.org/10.1111/clr.12805

Demirkol, A., Demirkol, M. O., Demirel, K., Meric, H., & Cantez, S. (2001). Blood flow of free gingival grafts measured by xenon-133 clearance. *Periodontal Clin Investig*, *23*, 15–19.

Firkova, E., & Bouka, M. (2019). Laser doppler flowmetry in the evaluation of periodontal health and disease. *J of IMAB*, *25*, 2599–2602. https://doi.org/10.5272/jimab.2019253.2599

Fleischer, A. C., Wojcicki, W. E., Donnelly, E. F., Pickens, D. R., Thirsk, G., Thurman, G. B., & Hellerqvist, C. G. (1999). Quantified color Doppler sonography of tumor vascularity in an animal model. *Journal of Ultrasound in Medicine*, *18*, 547–551. https://doi.org/10.7863/jum.1999.18.8.547

Fu, J. H., Hasso, D. G., Yeh, C. Y., Leong, D. J., Chan, H. L., & Wang, H. L. (2011). The accuracy of identifying the greater palatine neurovascular bundle: A cadaver study. *Journal of Periodontology*, *82*, 1000–1006. https://doi.org/10.1902/jop.2011.100619

Gao, J., Chevalier, J., Auh, Y. H., Rubin, J. M., Wang, H., Sun, L. N., Seshan, S., & Min, R. (2013). Correlation between Doppler parameters and renal cortical fibrosis in lupus nephritis: A preliminary observation. *Ultrasound in Medicine and Biology*, *39*, 275–282. https://doi.org/10.1016/j.ultrasmedbio.2012.10.009

Goddi, A., Fanizza, M., Bortolotto, C., Raciti, M. V., Fiorina, I., He, X., Du, Y., & Calliada, F. (2017). Vector flow imaging techniques: An innovative ultrasonographic technique for the study of blood flow. *Journal of Clinical Ultrasound*, *45*, 582–588. https://doi.org/10.1002/jcu.22519.

Hansen, K. L., Nielsen, M. B., & Jensen, J. A. (2017). Vector velocity estimation of blood flow – A new application in medical ultrasound. *Ultrasound*, *25*, 189–199. https://doi.org/10.1177/1742271X17713353

Hashim, D., Cionca, N., Combescure, C., & Mombelli, A. (2018). The diagnosis of peri-implantitis: A systematic review on the predictive value of bleeding on probing. *Clin Oral Implants Res*, *29*(Suppl 16), 276–293. https://doi.org/10.1111/clr.13127

Hernandez-Andrade, E., Jansson, T., Figueroa-Diesel, H., Rangel-Nava, H., Acosta-Rojas, R., & Gratacos, E. (2007). Evaluation of fetal regional cerebral blood perfusion using power Doppler ultrasound and the estimation of fractional moving blood volume. *Ultrasound in Obstetrics and Gynecology*, *29*, 556–561. https://doi.org/10.1002/uog.4005

Hernandez-Andrade, E., Jansson, T., Ley, D., Bellander, M., Persson, M., Lingman, G., & Marsal, K. (2004). Validation of fractional moving blood volume measurement with power Doppler ultrasound in an experimental sheep model. *Ultrasound in Obstetrics and Gynecology*, *23*, 363–368. https://doi.org/10.1002/uog.1002

Hernandez-Andrade, E., Thuring-Jonsson, A., Jansson, T., Lingman, G., & Marsal, K. (2004). Fractional moving blood volume estimation in the fetal lung using power Doppler ultrasound: A reproducibility study. *Ultrasound in Obstetrics and Gynecology*, *23*, 369–373. https://doi.org/10.1002/uog.1003

Hock, J. (1979). Vascular morphology in noninflamed healed gingiva of dogs. *Journal of Clinical Periodontology*, *6*, 37–44. https://doi.org/10.1111/j.1600-051x.1979.tb02289.x

Hock, J. M., & Kim, S. (1987). Blood flow in healed and inflamed periodontal tissues of dogs. *Journal of Periodontal Research*, *22*, 1–5. https://doi.org/10.1111/j.1600-0765.1987.tb01532.x

Kaplan, M. L., Jeffcoat, M. K., & Goldhaber, P. (1982). Blood flow in gingiva and alveolar bone in beagles with periodontal disease. *Journal of Periodontal Research*, *17*, 384–389. https://doi.org/10.1111/j.1600-0765.1982.tb01169.x

Keane, P. A., & Sadda, S. R. (2010). Imaging chorioretinal vascular disease. *Eye (Lond)*, *24*, 422–427. https://doi.org/10.1038/eye.2009.309

Kennedy, J. E. (1974). Effect of inflammation on collateral circulation of the gingiva. *Journal of Periodontal Research*, *9*, 147–152. https://doi.org/10.1111/j.1600-0765.1974.tb00666.x

Kuraji, R., Wu, Y. H., Hashimoto, S., Mishiro, S., Maeda, Y., Miyashita, Y., Ito, H., Miwa, Y., Sunohara, M., Kapila, Y., & Numabe, Y. (2020). Temporal and dynamic changes in gingival blood flow during progression of ligature-induced periodontitis. *Oral Diseases*, *26*(6), 1292–1301. https://doi.org/10.1111/odi.13328

Lai, P. K., Wang, Y. A., & Welsh, A. W. (2010). Reproducibility of regional placental vascularity/perfusion measurement using 3D power Doppler. *Ultrasound in Obstetrics and Gynecology*, *36*, 202–209. https://doi.org/10.1002/uog.7608

Levy, B. I., Schiffrin, E. L., Mourad, J. J., Agostini, D., Vicaut, E., Safar, M. E., & Struijker-Boudier, H. A. (2008). Impaired tissue perfusion: A pathology common to hypertension, obesity, and diabetes mellitus. *Circulation*, *118*, 968–976. https://doi.org/10.1161/CIRCULATIONAHA.107.763730

Mavropoulos, A., Aars, H., & Brodin, P. (2001). The acute effects of smokeless tobacco (snuff) on gingival blood flow in man. *Journal of Periodontal Research*, *36*, 221–226. https://doi.org/10.1034/j.1600-0765.2001.036004221.x

Molnar, B., Molnar, E., Fazekas, R., Ganti, B., Mikecs, B., & Vag, J. (2019). Assessment of palatal mucosal wound healing following connective-tissue harvesting by laser speckle contrast imaging: An observational case series study. *Int J Periodontics Restorative Dent*, *39*, e64–e70. https://doi.org/10.11607/prd.3878

Mormann, W., Bernimoulin, J. P., & Schmid, M. O. (1975). Fluorescein angiography of free gingival autografts. *Journal of Clinical Periodontology*, *2*, 177–189. https://doi.org/10.1111/j.1600-051x.1975.tb01740.x

Mormann, W., & Ciancio, S. G. (1977). Blood supply of human gingiva following periodontal surgery. *A Fluorescein Angiographic Study. J Periodontol*, *48*, 681–692. https://doi.org/10.1902/jop.1977.48.11.681

Newman, J. S., Adler, R. S., Bude, R. O., & Rubin, J. M. (1994). Detection of soft-tissue hyperemia: Value of power Doppler sonography.

AJR. American Journal of Roentgenology, *163*, 385–389. https://doi.org/10.2214/ajr.163.2.8037037

Oglat, A. A., Matjafri, M. Z., Suardi, N., Oqlat, M. A., Abdelrahman, M. A., & Oqlat, A. A. (2018). A review of medical doppler ultrasonography of blood flow in general and especially in common carotid artery. *J Med Ultrasound*, *26*, 3–13. https://doi.org/10.4103/JMU.JMU_11_17

Patino-Marin, N., Martinez, F., Loyola-Rodriguez, J. P., Tenorio-Govea, E., Brito-Orta, M. D., & Rodriguez-Martinez, M. (2005). A novel procedure for evaluating gingival perfusion status using laser-Doppler flowmetry. *Journal of Clinical Periodontology*, *32*, 231–237. https://doi.org/10.1111/j.1600-051X.2005.00655.x

Perussolo, J., Souza, A. B., Matarazzo, F., Oliveira, R. P., & Araujo, M. G. (2018). Influence of the keratinized mucosa on the stability of peri-implant tissues and brushing discomfort: A 4-year follow-up study. *Clin Oral Implants Res*, *29*, 1177–1185. https://doi.org/10.1111/clr.13381

Pinter, S. Z., Kripfgans, O. D., Treadwell, M. C., Kneitel, A. W., Fowlkes, J. B., & Rubin, J. M. (2018). Evaluation of umbilical vein blood volume flow in preeclampsia by angle-independent 3D sonography. *Journal of Ultrasound in Medicine*, *37*, 1633–1640. https://doi.org/10.1002/jum.14507

Renvert, S., Persson, G. R., Pirih, F. Q., & Camargo, P. M. (2018). Peri-implant health, peri-implant mucositis, and peri-implantitis: Case definitions and diagnostic considerations. *Journal of Clinical Periodontology*, *45*(Suppl 20), S278–S285. https://doi.org/10.1111/jcpe.12956

Retzepi, M., Tonetti, M., & Donos, N. (2007). Comparison of gingival blood flow during healing of simplified papilla preservation and modified Widman flap surgery: A clinical trial using laser Doppler flowmetry. *Journal of Clinical Periodontology*, *34*, 903–911. https://doi.org/10.1111/j.1600-051X.2007.01119.x

Roccuzzo, M., Grasso, G., & Dalmasso, P. (2016). Keratinized mucosa around implants in partially edentulous posterior mandible: 10-year results of a prospective comparative study. *Clin Oral Implants Res*, *27*, 491–496. https://doi.org/10.1111/clr.12563

Rubin, J. M., Adler, R. S., Fowlkes, J. B., Spratt, S., Pallister, J. E., Chen, J. F., & Carson, P. L. (1995). Fractional moving blood volume: Estimation with power Doppler US. *Radiology*, *197*, 183–190. https://doi.org/10.1148/radiology.197.1.7568820

Rubin, J. M., Bude, R. O., Carson, P. L., Bree, R. L., & Adler, R. S. (1994). Power Doppler US: A potentially useful alternative to mean frequency-based color Doppler US. *Radiology*, *190*, 853–856. https://doi.org/10.1148/radiology.190.3.8115639

Rubin, J. M., Bude, R. O., Fowlkes, J. B., Spratt, R. S., Carson, P. L., & Adler, R. S. (1997). Normalizing fractional moving blood volume estimates with power Doppler US: Defining a stable intravascular point with the cumulative power distribution function. *Radiology*, *205*, 757–765. https://doi.org/10.1148/radiology.205.3.9393532

Sculean, A., Gruber, R., & Bosshardt, D. D. (2014). Soft tissue wound healing around teeth and dental implants. *Journal of Clinical Periodontology*, *41*(Suppl 15), S6–S22. https://doi.org/10.1111/jcpe.12206

Stevenson, G. N., Collins, S. L., Welsh, A. W., Impey, L. W., & Noble, J. A. (2015). A technique for the estimation of fractional moving blood volume by using three-dimensional power Doppler US. *Radiology*, *274*, 230–237. https://doi.org/10.1148/radiol.14132363

Tatarakis, N., Gkranias, N., Darbar, U., & Donos, N. (2018). Blood flow changes using a 3D xenogeneic collagen matrix or a subepithelial connective tissue graft for root coverage procedures: A pilot study. *Clin Oral Investig*, *22*, 1697–1705. https://doi.org/10.1007/s00784-017-2261-5

Tattan, M., Sinjab, K., Lee, E., Arnett, M., Oh, T. J., Wang, H. L., Chan, H. L., & Kripfgans, O. D. (2019). Ultrasonography for chairside evaluation of periodontal structures: A pilot study. *Journal of Periodontology*, *91*(7), 890–899. https://doi.org/10.1002/JPER.19-0342

Tavelli, L., Asa'ad, F., Acunzo, R., Pagni, G., Consonni, D., & Rasperini, G. (2018). Minimizing patient morbidity following palatal gingival harvesting: A randomized controlled clinical study. *Int J Periodontics Restorative Dent*, *38*, e127–e134. https://doi.org/10.11607/prd.3581

Tavelli, L., Barootchi, S., Avila-Ortiz, G., Urban, I. A., Giannobile, W. V., & Wang, H. L. (2020). Peri-implant soft tissue phenotype modification and its impact on peri-implant health: A systematic review and network meta-analysis. *Journal of Periodontology*, *92*, 21–44. https://doi.org/10.1002/JPER.19-0716

Tavelli, L., Barootchi, S., Namazi, S. S., Chan, H. L., Brzezinski, D., Danciu, T., & Wang, H. L. (2020). The influence of palatal harvesting technique on the donor site vascular injury: A split-mouth comparative cadaver study. *Journal of Periodontology*, *91*, 83–92. https://doi.org/10.1002/JPER.19-0073

Tavelli, L., Barootchi, S., Ravida, A., Oh, T. J., & Wang, H. L. (2019). What is the safety zone for palatal soft tissue graft harvesting based on the locations of the greater palatine artery and foramen? A systematic review. *Journal of Oral and Maxillofacial Surgery*, *77*, 271.e1–271.e9. https://doi.org/10.1016/j.joms.2018.10.002

Tavelli, L., Ravida, A., Saleh, M. H. A., Maska, B., Del Amo, F. S., Rasperini, G., & Wang, H. L. (2019). Pain perception following epithelialized gingival graft harvesting: A randomized clinical trial. *Clin Oral Investig*, *23*, 459–468. https://doi.org/10.1007/s00784-018-2455-5

Vosborg, F., Malmqvist, L., & Hamann, S. (2020). Non-invasive measurement techniques for quantitative assessment of optic nerve head blood flow. *European Journal of Ophthalmology*, *30*, 235–244. https://doi.org/10.1177/1120672119858891

Welsh, A. (2004). Quantification of power Doppler and the index 'fractional moving blood volume' (FMBV). *Ultrasound in Obstetrics and Gynecology*, *23*, 323–326. https://doi.org/10.1002/uog.1037

Welsh, A. W., Fowlkes, J. B., Pinter, S. Z., Ives, K. A., Owens, G. E., Rubin, J. M., Kripfgans, O. D., Looney, P., Collins, S. L., & Stevenson, G. N. (2019). Three-dimensional US fractional moving blood volume: Validation of renal perfusion quantification. *Radiology*, *293*, 460–468. https://doi.org/10.1148/radiol.2019190248

Yousefi, S., Qin, J., Dziennis, S., & Wang, R. K. (2014). Assessment of microcirculation dynamics during cutaneous wound healing phases in vivo using optical microangiography. *Journal of Biomedial Optics*, *19*, 76015. https://doi.org/10.1117/1.JBO.19.7.076015

Zucchelli, G., Mazzotti, C., Mounssif, I., Marzadori, M., & Stefanini, M. (2013). Esthetic treatment of peri-implant soft tissue defects: A case report of a modified surgical-prosthetic approach. *Int J Periodontics Restorative Dent*, *33*, 327–335. https://doi.org/10.11607/prd.1632.

Zucchelli, G., Tavelli, L., Stefanini, M., Barootchi, S., Mazzotti, C., Gori, G., & Wang, H. L. (2019). Classification of facial peri-implant soft tissue dehiscence/deficiencies at single implant sites in the esthetic zone. *Journal of Periodontology*, *90*, 1116–1124. https://doi.org/10.1002/JPER.18-0616

SUPPORTING INFORMATION

Additional supporting information may be found online in the Supporting Information section.

How to cite this article: Tavelli L, Barootchi S, Majzoub J, et al. Ultrasonographic tissue perfusion analysis at implant and palatal donor sites following soft tissue augmentation: A clinical pilot study. *J Clin Periodontol*. 2021;48:602–614. https://doi.org/10.1111/jcpe.13424